

# INVESTIGATION OF THE STIFFNESS OF A SPECIALLY STRENGTHENED BRIDGE WHEN CROSSED BY VERY HEAVY VEHICLES – A CASE STUDY

---

**CZESŁAW MACHELSKI, MACIEJ HILDEBRAND\*,  
MAKSYMILIAN KLIŃSKI**

*Faculty of Civil Engineering, Wrocław University of Science and Technology,  
Wrocław, Poland*

Received 31 August 2023; accepted 15 December 2023

**Abstract.** The measurement of bridge deflection induced by a motor vehicle is an effective way of verifying the weight of the vehicle, and even of determining the layout of its axles. If the vehicle's weight and the impacts of its individual axles are known, deflection measurements can be used to verify the stiffness of the bridge structure and to evaluate the effectiveness of steel-concrete composite span integration. The bridge in this case study had been specially permanently adapted to carrying very heavy loads, generated by overweight transports reaching the total weight of a few to over 10 MN. The results of measurements of span deflections induced by a heavy vehicle and the way they were used to assess the weight of another overweight transport unit crossing the bridge are presented in the paper. The existing strengthening of the bridge has been found to be universal and effective for various overweight transports.

**Keywords:** deflection measurement, overweight transport, road bridge, strengthening, weigh-in-motion.

---

\* Corresponding author. E-mail: [maciej.hildebrand@pwr.edu.pl](mailto:maciej.hildebrand@pwr.edu.pl)

Czesław Machelski (ORCID ID 0000-0002-1215-7908)  
Maciej Hildebrand (ORCID ID 0000-0001-8011-2464)  
Maksymilian Kliński (ORCID ID 0000-0002-9509-2440)

Copyright © 2024 The Author(s). Published by RTU Press

This is an Open Access article distributed under the terms of the Creative Commons Attribution License (<http://creativecommons.org/licenses/by/4.0/>), which permits unrestricted use, distribution, and reproduction in any medium, provided the original author and source are credited.

## Introduction – heavy vehicles in road transport

Road bridges are subjected from time to time to very high loads by some heavy goods vehicles. For small-span bridges compact four-axle vehicles, often characterized by small inter axle spacing (as illustrated in Figure 1), are particularly stressful. Vehicle sets or special vehicles with a large number of axles, despite their heavy weight, in many cases do not

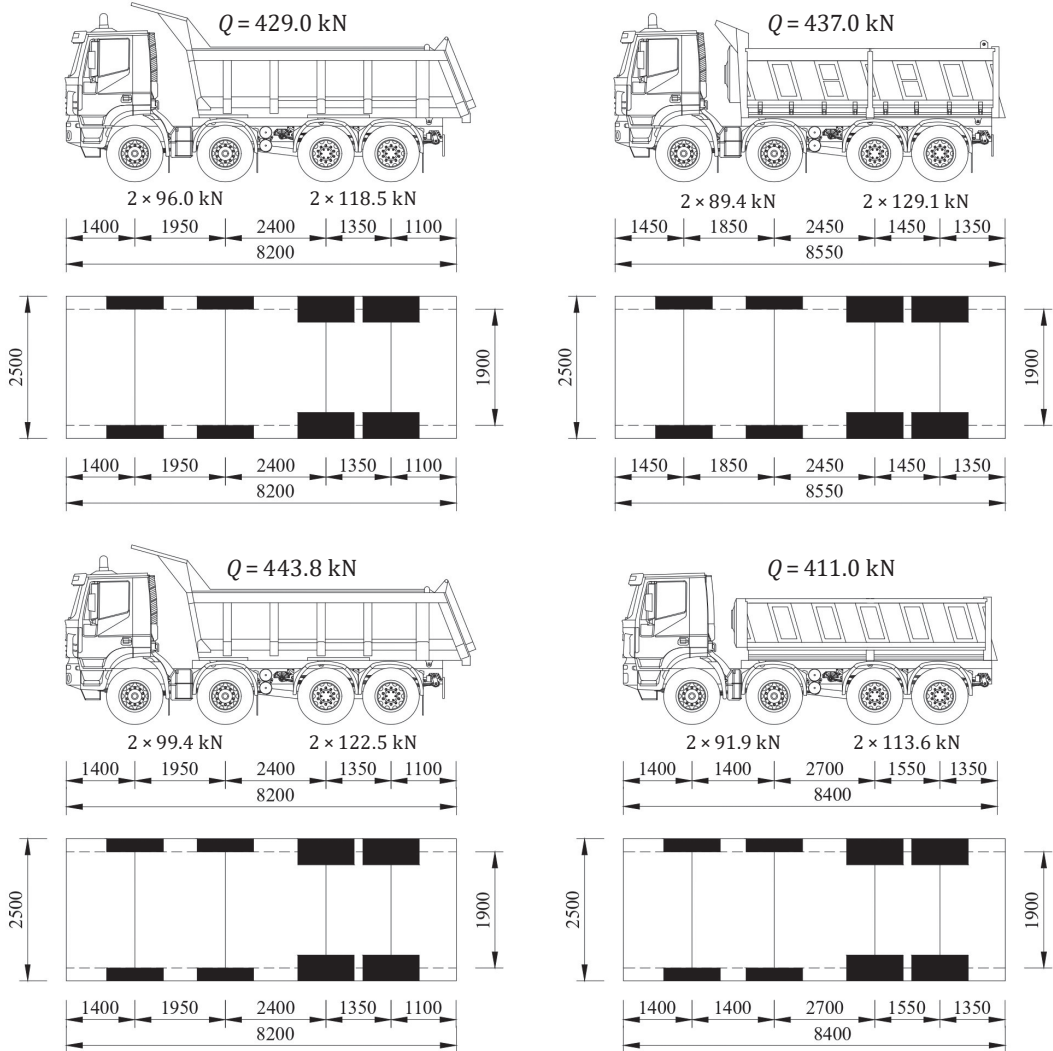


**Figure 1.** Examples of actual four-axle T4 lorries with small inter axle spacing (formally overloaded)

constitute very heavy loads as only a part of the whole vehicle (or of a vehicle set) can fit on a bridge.

In the case of small bridges an adverse situation occurs when two heavy and short vehicles pass each other on a bridge. The total weight of two T4 lorries amounts to:  $Q = 2 \times 443.8 = 888 \text{ kN}$  (see Figure 1), and so it is close to that of the lighter oversize road transports considered further on. Such an adverse loading configuration occurs rather seldom, but it may result in full bearing capacity mobilisation, which is discussed later in this paper. (It should be added that vehicles presented in Figure 1 are formally overloaded).

Concerning large-span road bridges, a congestion on a bridge significantly impacts its loading. Then motor vehicles, whose weight and arrangement are random, are concentrated on the bridge roadway at a minimal spacing, as in Figure 2. From the point of view of bridge loading, the fact that in the case of a traffic congestion, dynamic impacts are completely reduced (due to the minimal speed of movement of the vehicles) is beneficial. The arrangement of the vehicles may result in a vehicles accumulation amounting to great total vehicle weight (Machelski & Hildebrand, 2021). This is done on purpose in bridge acceptance tests during which heavy lorries with great, but controlled weight are positioned on the bridge.

This paper considers special transports of very heavy goods conducted using special tractor (towing vehicle) combined with trailer (some other examples of such vehicle sets are presented in Figure 3), or self-propelled trailers. In the case of small- and medium-span bridges the loading system, comprising a considerable number of axles, occupies the entire length of the bridge, but not all of it fits on the bridge, whereby it is less stressful than in the case of large-span bridges. Transports whose



**Figure 2.** Congestion on the roadway of a cable-stayed bridge

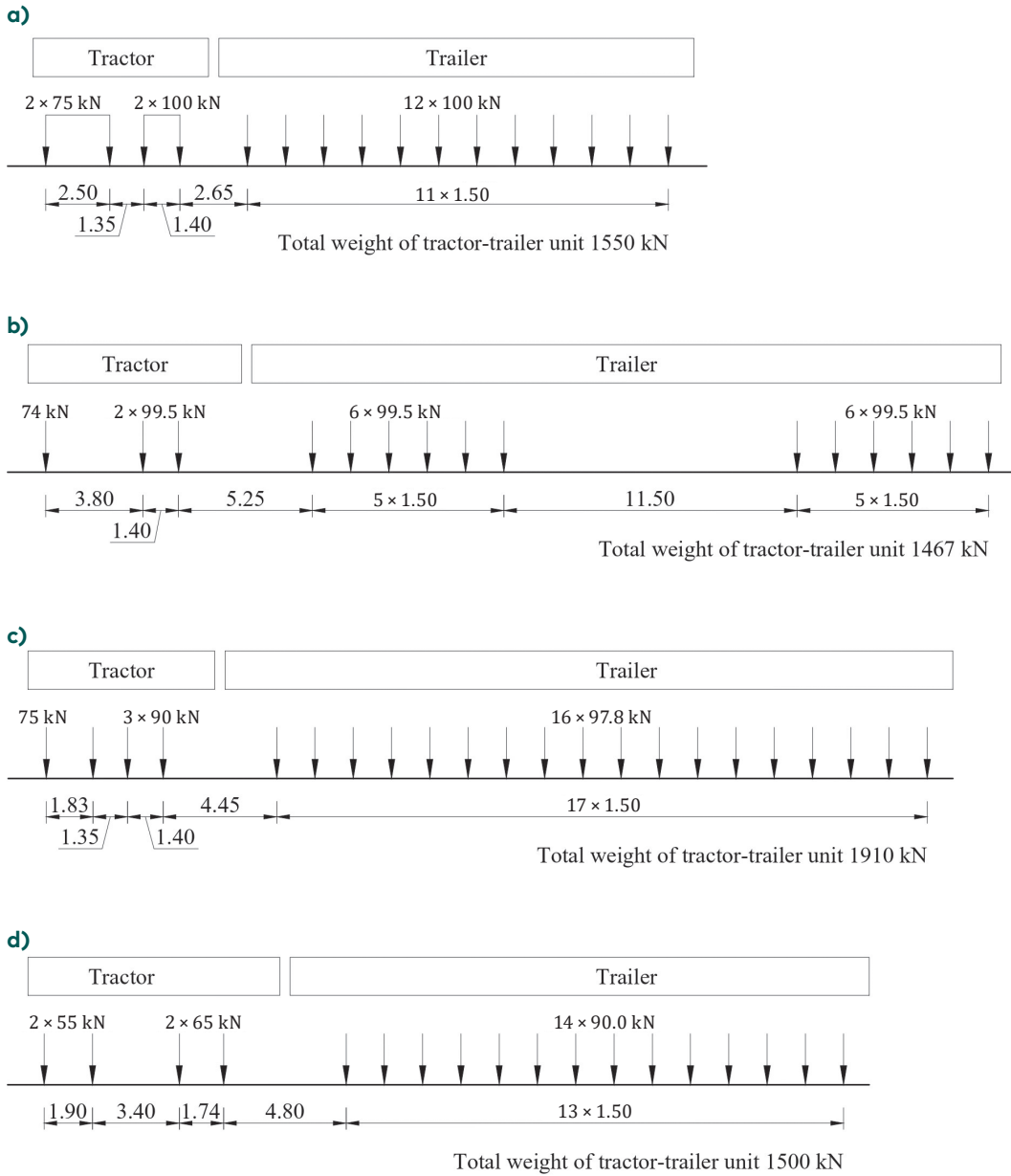


**Figure 3.** Exemplary abnormal tractor-trailer units with different arrangements of tractor and trailer axles, other than considered in this paper

size or weight is greater than a certain limit is treated as abnormal and then it is the only vehicle on the bridge (during an escorted crossing) and in addition, it moves very slowly on the central axis of the roadway. The aim of the speed limitation in this case is to reduce dynamic impacts.

A cargo carrying semitrailer, or a trailer is pulled by a tractor and if necessary, pushed by a pusher vehicle situated at the back of the set of vehicles. Such a system together with the transported heavy cargo, e.g., a transformer, can reach weight even 4000 kN. A configuration of abnormal vehicles set, the number of axles and the loads exerted by it onto the deck are matched so as not to exceed the bridge's live load capacity.

Exceptionally special transports for which bridges have not been designed are carried out. They are conducted using special vehicles being self-propelled sets of slow-moving axles. In the considered case,



**Figure 4.** Abnormal transport of gas turbine on special vehicle with its own drive (self-propelled trailer)

the bridge had been permanently strengthened so that it could carry various abnormal transports.

The considered bridge is located on a route leading to an industrial plant where new process equipment is being installed as part of upgrading. Loads of considerable size and weight are delivered by water on a barge to a riverside and then reloaded onto vehicles. Figure 4 shows an example of a special transport (the conveyance of a gas turbine on a self-propelled trailer). Unlike road transports comprising a tractor and a special trailer, the vehicle presented above has its own drive and an independent control of each of its wheels, whereby it can precisely fit into the curvature of a road route, which is vital especially in the case of very long sets of axles.

## 1. Issues relating to abnormal transports

Investigations on abnormal road transports are conducted in various countries (Gnap et al., 2022; Godavarthy et al., 2016; Hammada et al., 2013; Macioszek, 2020, Mohammed et al., 2018, Petru & Krivda, 2017, Petru & Krivda, 2021, Vrabel et al., 2022, Wood et al., 2007; Yudhistira et al., 2022). According to the data reported in (Petru & Krivda, 2021), the weight of abnormal transports most often amounts to about 100 t (1000 kN). Transports weighing about 350–450 t (3500–4500 kN) occur rather sporadically. Study (Onysyk & Hildebrand, 1999) analyses cases of abnormal transports weighing from 100 to 170 t (1000–1700 kN) and concludes that in the considered situations despite their considerable weight the heavy vehicles did not induce in the spans internal forces significantly greater than the standard loads for which the bridges had been designed. This observation was based on a comparative analysis of the internal forces generated in selected cross sections of the spans by respectively the standard loads and the loads declared by companies conducting the abnormal transportation. It was also suggested that transports weighing as much as 400 t (4000 kN) could be exceptionally run on public roads, including on bridges designed for standard loads. An extensive analysis of abnormal loads observed mainly in Slovakia was presented in (Gnap et al., 2022). Statistical analyses of loads were performed. Information about the actual technical condition of bridge structures is also provided. Some legal aspects of issuing permits for non-standard transports were presented, including relevant legal documents. The idea of a global approach instead of the current local approach (i.e., individual analysis of each bridge) and the use of an application allowing for modifying the individual need to obtain permits for the passage of transports weighing up to 120 t and height up to 4.5 m

on selected routes, selecting the appropriate route and type of vehicle for planned non-standard transport are also presented. It should be noted here that a bridge crossing by a vehicle with the total weight of over 1000 t (10 000 kN) is analysed in the present paper.

The work (Hammada et al., 2013) presents an analysis of the impact of heavy loads (with a mass of over 330 t) on a specific bridge structure, curved in plan with a steel structure, located in Oregon in the USA. The cited article presents a procedure for assessing the behaviour of a bridge and the safety of non-standard transport, starting with measurements of structure deformations under a known load. The obtained results made it possible to specify the mechanical characteristics of the bridge, i.e., calibrate the FEM model, which was helpful in determining the structural effort during planned non-standard transports and allowed for reliable monitoring of the structure during planned non-standard transports.

A very thorough analysis of the impact of heavy vehicles on steel and concrete bridge spans is given in the study (Wood et al., 2007). This analysis concerns both the immediate and long-term effects of the impact of abnormal vehicles on bridges in Indiana, USA. The main conclusions refer among others to finding the weak points of bridges when analysing the influence of heavy load on the structure and question on influence of heavy load passage on fatigue of superstructure. It was found that this influence was rather moderate or even negligible.

The case of a bridge with a traditional wooden structure, through which non-standard transport had to be carried out, related to the construction of a power plant on the island of Borneo in Indonesia, is analysed in (Yudhistira et al., 2022). The bridge was built in the forest, from tree trunks (log bridge) and it was proposed to rebuild it by reducing the span and placing additional tree trunks and modifying the abutments. However, the bridge span still had a traditional structure, i.e., it was composed of wooden logs supplemented with soil filling. It has been shown that by using handy, available materials, the problem of transporting a load weighing over 100 t over a wooden bridge with a span of about 20 m can be solved. The described bridge was subjected to numerical analysis and field tests.

The work (Vrabel et al., 2022) analyses the lateral forces generated during the transport of a heavy load caused by its inertia and surface disturbances, including disturbances on expansion joint devices and on the bridge spans themselves. However, the issues of load-bearing capacity of bridge spans loaded with very heavy vehicles are not analysed.

The issue of non-standard transport is also considered in the work (Mohammed et al., 2018). This time, the authors' attention is focused on the dynamic "amplification" of the bridge load during non-standard

crossing due to regular spacing between the axles moving at low speed, and thus the occurrence of rhythmic load, which may lead to a coincidence with the natural frequency of the bridge. The cited work describes in detail the dynamic models of the interaction of vehicles and bridges. The conclusion states that in the analysed cases, e.g., when the set moves at a speed of approximately 30 km/h, a clear dynamic excitation may occur, significantly increasing the effort of the bridge structure.

In several publications, attention is paid to the geometrical aspects of conducting abnormal transports or to its economic aspects, and to a lesser extent to issues relating to the load-bearing capacity of bridges loaded with extremely heavy transport units. Particularly studies (Petru & Krivda, 2017; 2021) indicate difficulties involved in the passage of abnormal transports through sharp bends, intersections and streets equipped with public transport overhead catenary systems. It is indicated that there is a need to model such a passage using the Global Navigation Satellite System (GNSS).

The geometrical aspects of running abnormal transports are analysed in detail in paper (Godavarthy et al., 2016) in which issues relating to their passage through roundabouts are considered and the necessity to model such a passage by means of appropriate computer tools is indicated. The attention is focused mainly on issues relating to long transport units (used, e.g., for transporting wind turbine blades), whereas the weight of the abnormal transport units and its impact on the structural members of bridges is not examined.

It should be noted that guidelines for abnormal transports (European Guidelines, 2006) have been drawn up in the EU. The document includes comments concerning both abnormal transport management (e.g., obtaining permits) and practical guidelines for conducting such transports, concerning, e.g., escorting abnormal transport units. Also, information about abnormal vehicles, (among which heavy trailers and semitrailers and self-propelled vehicles or self-propelled trailers are distinguished), is provided. It is indicated that the largest “standard” transport units can weigh up to 72 t (720 kN), their axle load can amount up to 15 t (150 kN) and their length up to 20 m (Section 8 in (European Guidelines, 2006)). Any cases of transport units of greater weight or size require a special permit. The transports described in the present paper are such cases.

The problem presented in this paper can, at least partially, be attributed to the area of weigh-in-motion research. The weigh-in-motion is well-known methodology (for instance: Helmi et al., 2014; Lydon et al., 2016) and it is used for measuring bridge deflections and determining the axle loads of vehicles on this basis.

It should be noted that this methodology is used for standard vehicles (typical lorries), whereas in the present paper a special version of the weigh-in-motion methodology is applied to abnormal transports with extraordinarily great weight and axle loads.

Numerous studies concentrate on determining the variable loads induced by vehicular traffic on the bridge deck. One should note that in many cases the position and weight of a vehicle can be determined (both theoretically and practically) not only on a beam bridge (Helmi et al., 2014; Lydon et al., 2016), but also on a cable-stayed bridge (Machelski & Hildebrand, 2015; 2021), using structural health monitoring systems. The procedures being developed for this purpose are usually referred to as a weigh-in-motion technology, which implies that such measurements are performed as part of permanent monitoring (Hildebrand et al., 2008). The case presented in this paper refers to an incidental measurement project.

## **2. Bridge and its strengthening**

The considered bridge is located on the Brzeźnica River (near its outlet to the Vistula River) in Płock (Poland). The bridge is in everyday use in a network of city streets. The motor traffic is of low intensity and the pedestrian traffic is sporadic. Very heavy transports pass through the bridge as in its vicinity there is a road leading down to the Vistula and an industrial riverside for reloading cargo transported by waterway. Because of its location and way of use (for occasional conveyance of heavy loads) the bridge structure had been subjected to alterations:

- The deck had been strengthened by incorporating additional stringers;
- Two additional intermediate piers on separate pile foundations had been built in between the abutments;
- The abutments had been mutually strutted (stabilized) with steel struts.

The bridge's (Figure 5) specifications are as follows:

- The length of the steel structure 17.20 m;
- The theoretical length of the interior span 13.10 m;
- The length of the end spans 1.40 m and 2.30 m;
- The overall width of the deck 10.40 m;
- The centre-to-centre spacing of the main girders 1.15 m;
- The greatest height of the spans 1.15 m;
- The usable width of the roadway 7.00 m;
- The usable width of the sidewalks 2×1.5 m.

The bridge superstructure is made of steel beams HEB700. In its cross section there are eight beams at a c/c spacing of 1.15 m. The beams are braced together by lightweight lattice beams made of angles. A (probably) 17–19 cm thick concrete slab, thickened to about 40 cm at the sidewalks, constitutes the deck. There are no distinct separate walkway slabs. There are additional steel stringers between the main girders parallel to the latter, strengthening the deck against the heavy wheel loads of abnormal vehicles.

The main beams are stiffened over the end bearings (over the abutments) and in the places where there are cross beams. There are no stiffeners over the intermediate piers. The superstructure rests on the solid abutments and on the intermediate steel frame supports. There are tangent steel bearings on the left-bank abutment (the side leading to the city centre) and roller bearings on the right-bank abutment. There are very special tangent bearings made of packs of flat bars on the intermediate piers in order not to load the bearings over the intermediate piers under light operational load.

The frame-shaped intermediate piers are made of double-tee bars I 550 and other additional components and they are wholly welded. The piers rest on a reinforced concrete member joining the heads of the large-diameter piles together and performing the function of a cap and a tie. The piles had been drilled in the soil beyond the span's bird-view outline.



**Figure 5.** Bridge over Brzeznica in Płock: a) side view; b) view of span bottom, intermediate steel support, struts and abutment. Additional stringers are visible between main beams



were used. The sensors C&E are installed not exactly in the middle of the span, but under the cross-point of main girders and crossbeams of the span, as in this case there is no need to find the theoretical point of midspan in the field. Moreover, this way the deflections were measured in the points of structure's nodes.

#### 4. Bridge crossing by two-sets-of-axle special transport

The largest of the analysed abnormal transports was the transport of a wash tower placed on two sets of axles. An overview of the transport unit is shown in Figure 7 and its main specifications are given below:

- The wash tower with a total weight of  $2 \times 644.4 \text{ t}$  ( $2 \times 6444 \text{ kN}$ );
- The number of axles during bridge crossing:  $2 \times 18$ ;
- The total axle load during bridge crossing: up to  $37.2 \text{ t}$  ( $372 \text{ kN}$ );
- The axle spacing: 1.4 m in each of the two sets;
- The interval between the nearest axles of the successive sets: 17 m;
- The width of the vehicle at the level of its contact with the bridge deck surface: 5.33 m.

The cargo was weighed (as a check) during loading on the set of trailers. A weight measuring device operating on a crane was used to measure the total weight of the transported item. This way it was possible to compare the declared weight with actual one. It was found, that the weight of the biggest element (wash tower) described in this paper was slightly smaller than declared. It should be added, that for the heaviest loads, trailers are used with a hydraulic system that precisely balances the loads on all axles.

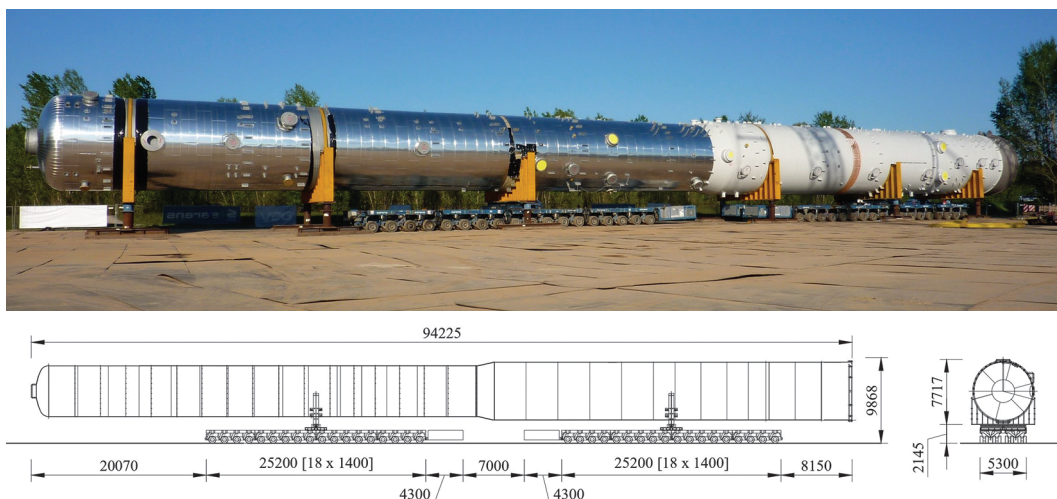
The bridge crossing by this special transport was preceded by detailed analyses of the route's geometry in order to rule out potential collisions with the road signs and lighting and the trees near the shoulder. A certain number of the trees had to be cut down. The collision problem was clearly apparent in this case considering the shape of the street before and after the bridge (a bend and a change in the road's grade line). It was essential to closely follow the planned course of passage of the transport unit's first element. The crossing took place at night on 9–10 May 2023.

Figure 8 shows the measured deflections. According to the graphs presented in Figure 8 the largest vertical displacements were registered in point C, i.e., 5.4 m from the right-bank steel pier (visible on the left side in Figure 6a). This deflection amounted to about 15.5 mm. The

largest registered deflection is not identical with the largest deflection which could be expected at the midspan of the central span, as the sensors were installed in the cross sections in which superstructure cross girders occurred. After the first group of axles crossed the bridge, a short pause followed during which there was no load on the bridge, which was registered at about 22:42 (see Figure 8). Then the second set of axles entered the bridge and its impacts were similar to those of the first set. After the whole transport unit exited the bridge, the sensors indicated small displacements of about 0.5 mm, which in the case of points B and C amounted to no more than 3% of the largest deflections. The residual deflections can be accepted without any reservations.

An analysis of the graphs presented in Figure 8 shows that after the first set of axles crossed the bridge a strain relief occurred as the interval between the first and second set of axles is approximately equal to the overall length of the spans. Thus, the load effects of the two sets of axles can be analysed separately. The small difference between the maximum deflections of point C, caused by the presence of the first set of axles and then the second set, can be due to the difference between the weight of the first element and that of the second element and also due to transversal dislocation of the second set of axles when compared to the first set.

Prior to its entrance onto the bridge, the abnormal transport unit moved on a horizontal curve because of the curvature of its route (a bend along the street). The first set of axles moved close to the kerb



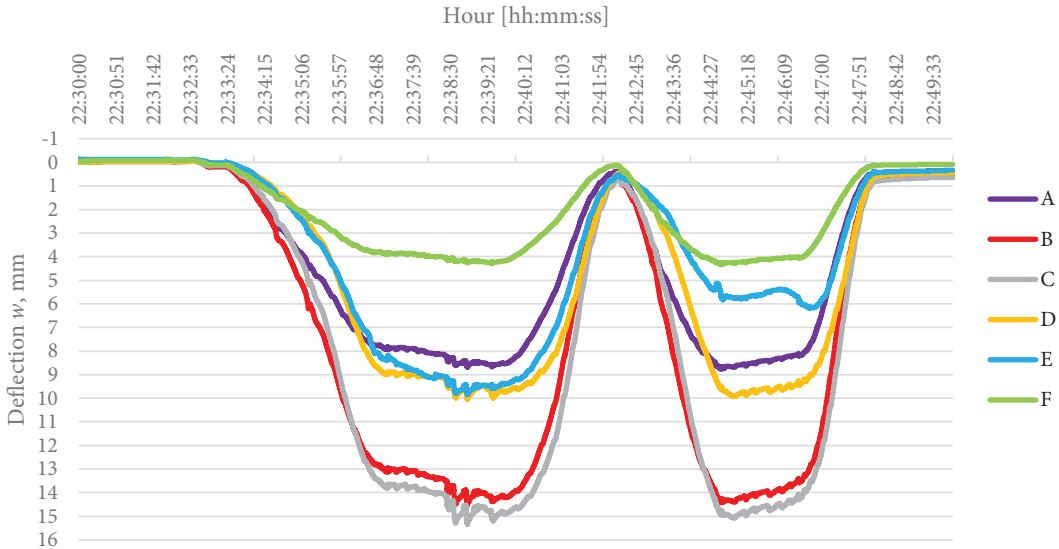
**Figure 7.** View and geometrical parameters of special transport (wash tower)

near beam no. 8 (on the outside of the curve), whereas the second set of axles moved close to the kerb near beam no. 1 (on the inside of the curve). Consequently, during the crossing of the first set of axles the edge beam (no. 8) was more loaded than during the crossing of the second set of axles. Figure 9 shows the positions of the load in the bridge's cross section during the passage of the transport unit. The position of the first group of axles is marked green while that of the second group of axles is marked blue. A shift of the loads relative to the axis of the bridge is visible.

The position of the vehicle (in the cross section of the span) is given by the ratio of the deflection of respectively point C and E, as a function of time ( $t$ ) as in the formula

$$r(t) = \frac{w_E(t)}{w_C(t)}. \quad (1)$$

Therefore, when the vehicle is shifted transversely towards edge girder no. 8 (and measuring point E), the value of  $w_C$  decreases while that of  $w_E$  increases at the same instant  $t$ . This means that function  $r(t)$  comprises the two changes in deflection. Figures 10–12 present selected fragments of the curve representing the change in the deflection of points C and E in time domain and the accompanying functions  $r(t)$ .



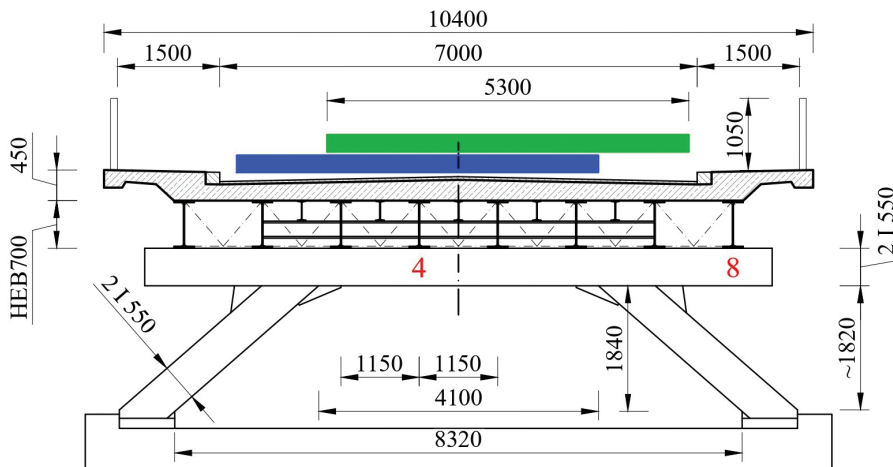
**Figure 8.** Graphs of deflections of points A, B, C, D, E, F during bridge crossing

Figure 10 presents changes in deflection during the passage of the first set of wheels when maximum deflections are reached in point C. A comparison of the graphs of deflections  $w_C(t)$  and  $w_E(t)$  and  $r(t)$  shows their great similarity.

Figure 11 presents changes in deflection again during the crossing of the first set of wheels, i.e., the first element of the vehicle, when deflection about 15.16 mm is reached in point C. A comparison of deflection graphs  $w_C(t)$  and  $r(t)$  shows their great similarity.

Local increases and decreases in deflections visible in Figures 10–12 are the result of subsequent trailer axles passing over the measurement site and in its surroundings. The disturbances in the deflection diagram visible locally in the graphs reach approximately 0.5–1 mm. The interval between the extremes of the deflection graph on the abscissa is approximately 20 s. Taking into account the distance between the trailer axles is 1.4 m, this means a speed of approximately 0.2–0.3 km/h. This was the average speed at which the analyzed non-normative set moved. The local disturbances of deflection over time curve are also due to relative horizontal movement of the trailer on the deck (due to curved line of its passage).

The irregular course of the deflection curve results from the numerous axles (and wheels) entering and leaving the bridge during the tests.



**Figure 9.** Position of load in bridge cross section during heavy transport passage over bridge. Main beams subjected to deflection tests are denoted with numbers 4 and 8

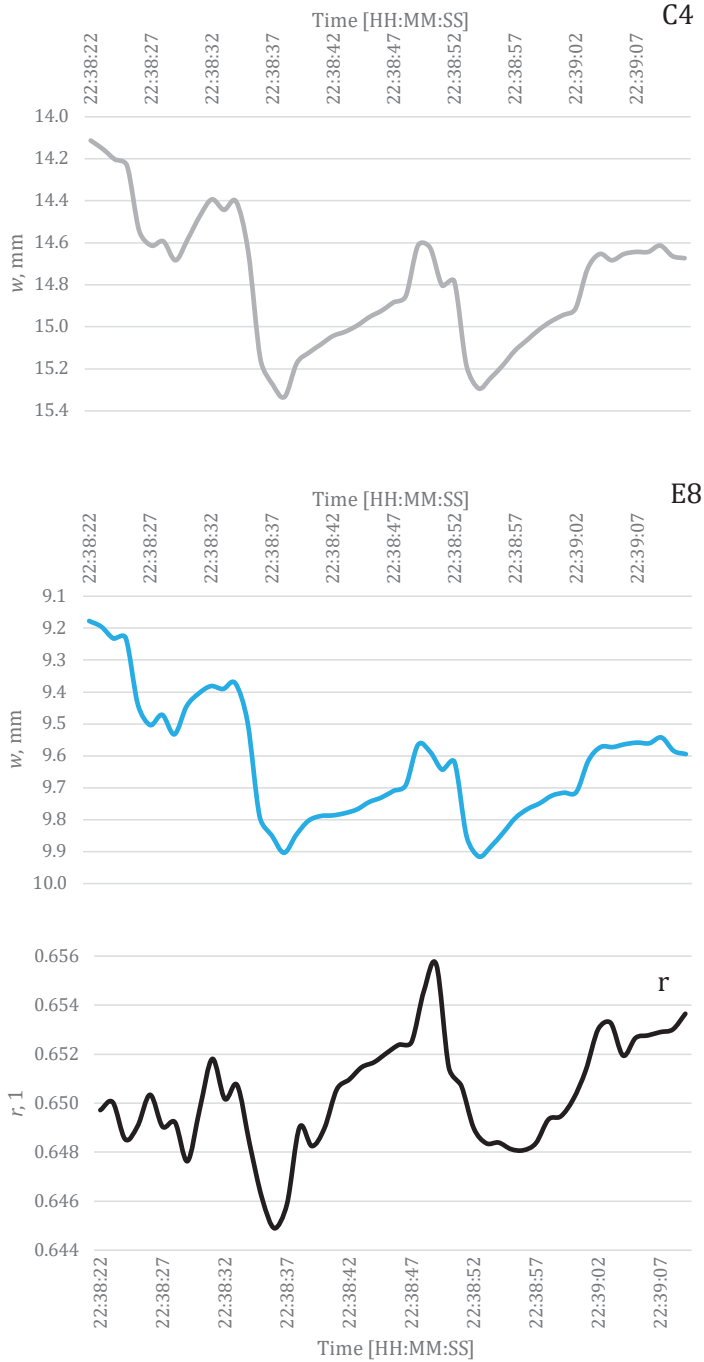


**Figure 10.** Local changes in deflection of points C and E during passage of first set of axles

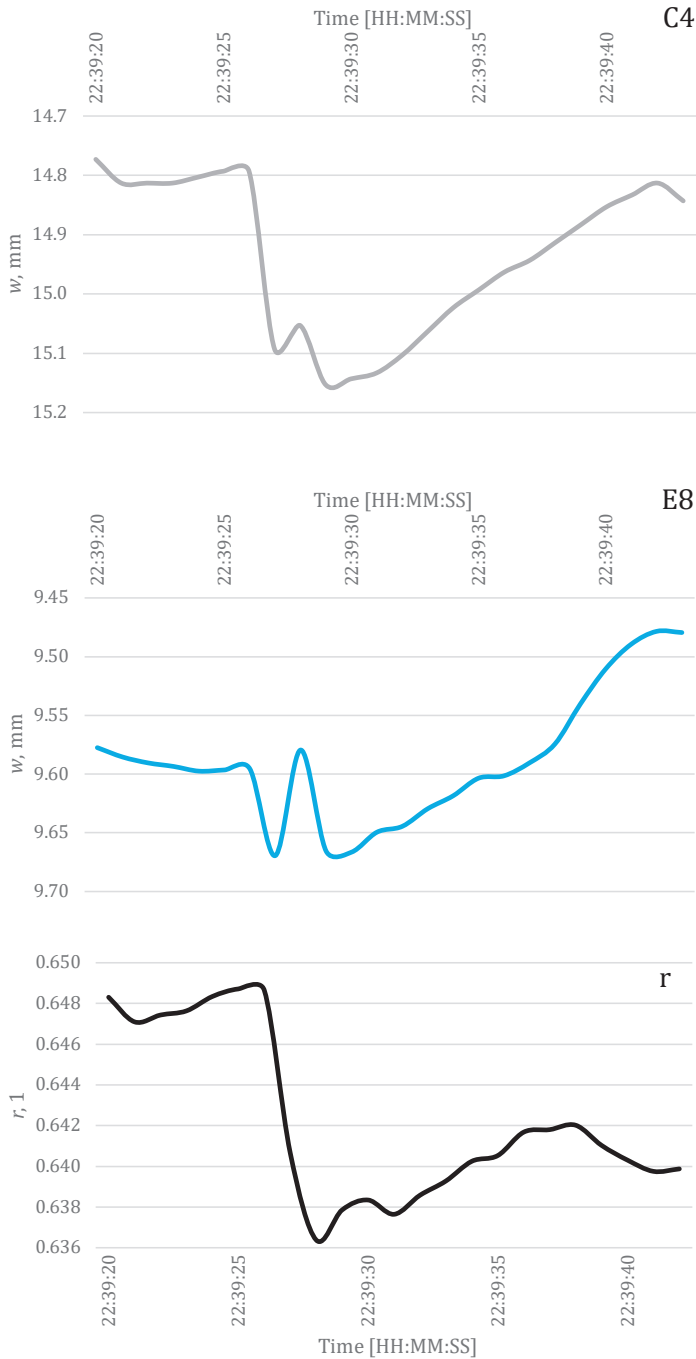


**Figure 11.** Local changes in deflection of points C and E during next phase of passage of the first set of axles

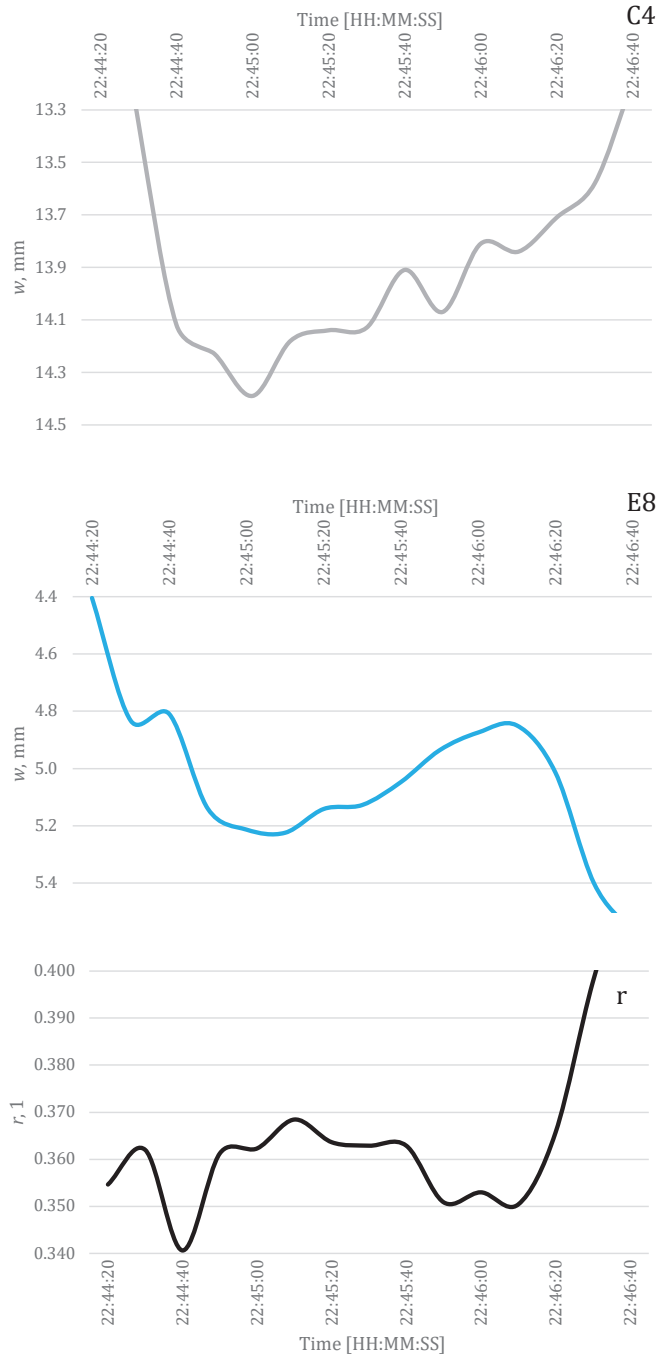


**Figure 12.** Local changes in deflection of points C and E during passage of the second set of wheels

After the first group of axles exited and the second group entered the bridge, the proportion of displacements of girder 8 (sensor E) changed relative to intermediate girder 4 (sensor C). The value of function  $r(t)$  indicates the opposite (relative to the road axis) positions of the two successive elements of the vehicle, which is shown in the loading diagram in Figure 9.

Figure 12 presents changes in deflection during the crossing of the second set of wheels, in selected time interval. The pattern of changes in deflection is generally similar to the previous ones. From the  $r(t)$  graphs presented in Figures 10–12 one can conclude that the effectiveness of the span's transverse bracings (shown in Figure 5b) is very low. In the face of clearly ununiform load distribution in the span cross section (directly under the abnormal vehicle), the contribution of the edge girder (no. 8) to load carrying during the passage of the first set of axles amounts to about  $r = 0.65$ . Maximally  $r$  would equal 1 if the load were evenly distributed over the whole span width and the bending of the whole span were cylindrical. In the case of the passage of the second set of axles, at a small difference in load position (visible in Figure 9),  $r = 0.36$ , which means that the contribution of girder no. 8 in load carrying decreases almost twice.

## 5. Calibration of the model of span

The results of the deflection measurements performed during the crossing of the bridge by the special transport were used in this study to develop a model of the bridge structure. The analysis was carried out for the span's beam no. 4 as in Figure 13. Measuring points A, B, C, D, F were located under this girder, as shown in Figure 6. When the vehicle's set of wheels covers the whole span, the load (in the form of several concentrated forces) is treated as a uniformly distributed force (load) with magnitude  $p$ , taking advantage of the fact that the vehicle wheel loads are effectively distributed thanks to the additional deck slab support elements (i.e., stringers) within the roadway area.

The shape of the line of beam deflection  $w(x)$  under load  $p$ , as shown in Figure 14, in the zone between points F and G (because of the limitations of the differential equation only segment FG is analysed below, but in reality, the load extends over the whole length of the beam) is interrelated with girder stiffness  $EI$  through the relation:

$$p = EI \frac{d^4 w}{dx^4}. \quad (2)$$

In a differential formulation (Orkisz, 1998) the relation assumes the form of the system of equations:

$$\left\{ \begin{array}{l} p = EI \frac{16}{c^4} (w_A - 4w_{AB} + 6w_B - 4w_{BC} + w_C) \\ p = EI \frac{16}{c^4} (w_{AB} - 4w_B + 6w_{BC} - 4w_C + w_{CD}) \\ p = EI \frac{16}{c^4} (w_B - 4w_{BC} + 6w_C - 4w_{CD} + w_D) \end{array} \right. \quad (3)$$

where  $c = 3.2$  m is the distance between the measuring points. Deflections  $w_A$ ,  $w_B$ ,  $w_C$  and  $w_D$  come from tests, while displacements  $w_{AB}$ ,  $w_{BC}$  and  $w_{CD}$  are intermediate values between measuring points A, B, C, D. They can be determined from the system of equations:

$$\begin{bmatrix} 4 & 4 & 0 \\ 1 & 6 & 1 \\ 0 & 4 & 4 \end{bmatrix} \cdot \begin{bmatrix} w_{AB} \\ w_{BC} \\ w_{CD} \end{bmatrix} = \begin{bmatrix} w_A + 6w_B + w_C \\ 4(w_B + w_C) \\ w_B + 6w_C + w_D \end{bmatrix}. \quad (4)$$

Based on Equation (4) one can determine the deflection at midspan, using the displacements measured in points A, B, C, D, from the Equation (5):

$$w_{BC} = \frac{1}{16} [9(w_B + w_C) - (w_A + w_D)]. \quad (5)$$

The essential issue of model presented in Figure 13 is to determine the flexibility of the support of the girder by the intermediate steel frame piers (compare Figures 5, 6, 13). For this purpose, a case when the load fully covered the span, and so could be treated as uniformly distributed load  $p$ , was analysed. The deflections of the girder over the frame supports are interrelated with the reactions caused by load  $p$  through stiffnesses  $k$  (in points F and G)

$$k_F = \frac{R_F}{w_F}, \quad (6)$$

and

$$k_G = \frac{R_G}{w_G}. \quad (7)$$

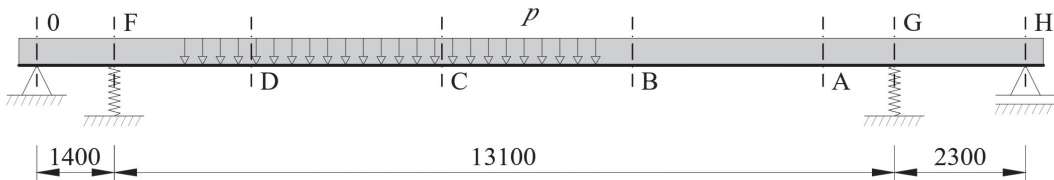


Figure 13. Load diagram of girder no. 4

Calculations done for the span model as in Figure 13 and function  $w(x)$  yielded stiffnesses:  $k_F = 81$  kN/mm and  $k_G = 110$  kN/mm. The calculations showed that the additional frame supports carry the loads caused by abnormal transport.

However, the flexible supports located in points F and G significantly reduce deflection. Without them the girder's maximum deflection would reach a two-and-a-half-fold higher maximum value:

$$w = \frac{5}{384} \frac{pL^4}{EI} = \frac{5 \times 44 \times 16.8^4}{384 \times 1207} = 37.8 \text{ mm.} \quad (8)$$

In order to formulate a girder (beam no. 4 and the other beams) model it is essential to determine bending stiffness  $EI$ . The measured deflections indicate that the steel girder is fully integrated with the reinforced concrete deck slab. Thus, this stiffness amounts to  $EI_z = 1207$  MNm<sup>2</sup>. By carrying out comparative analyses of the deflections calculated using the FE girder model and the ones measured for selected loading state, the line of deflection  $w(x)$  shown in Figure 14 was determined. The intensity with which one girder (no. 4) is loaded with uniformly distributed force  $p = 44$  kN/m was used for the calculations. Its value had been calculated taking into account the stipulated agreement between the results (for beam no. 4) of respectively measurements and calculations made using the model presented in Figure 13. From the assumption of the above value of distributed force  $p$  and from the relation:

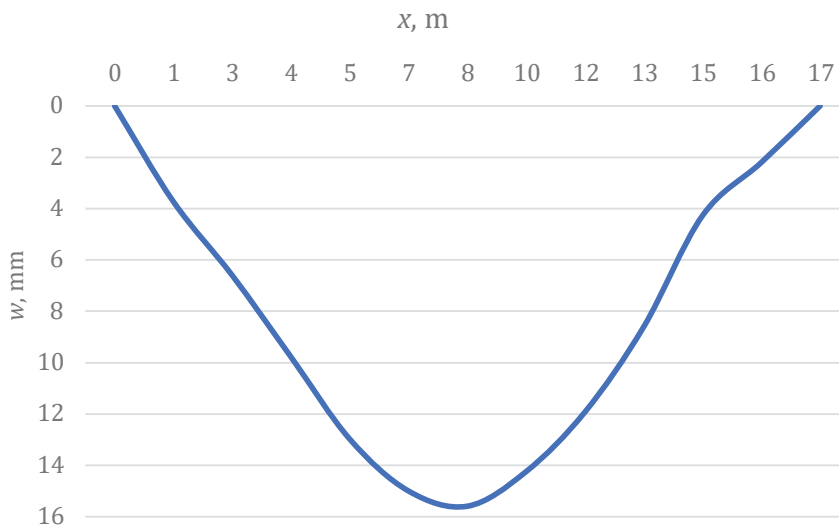


**Figure 14.** Line of deflection  $w(x)$  of beam no. 4

$$p = \frac{P}{n \cdot a} \quad (9)$$

follows the number of girders loaded identically as the considered girder:

$$n = \frac{P}{p \cdot a} = \frac{372}{44 \times 1.4} = 6.04. \quad (10)$$

In Equation (10)  $P$  is the axle load and  $a$  is the vehicle's spacing of axles. The  $r$  parameter values given in Figures 10–12 were used to calculate  $n$ .

Obviously, the permission for the transport company to pass the bridge which is the subject of the analysis was issued before all the results reported above were known, as the measurements were taken during the passage. The analysis of the bridge before issuing the passage permit was done independently by two engineers, working separately. The first one used the model and appropriate software and the second checked the effort of the structure under heavy loads without any computer, in simplified way. It was due to extremely heavy cargo and very high cost of transported element of industrial installation. The results were not exactly the same, but both lead to the same conclusion: the passage was possible and safe. There were the acceptable margins of safety in both analyses. Span deflection was considered a key parameter in the safety analysis in the light of the planned non-standard passage.

Predicting the deflections of the main girders during the passage of a heavy vehicle over the analyzed bridge structure was very difficult. This was mainly due to the question on the effectiveness of the cooperation of an additional steel support, as shown in Figure 5b, in carrying the loads appearing on the deck. The support was designed in the way, that under low loads (passenger cars) the frame would not participate in carrying the loads of the span. This was realized by leaving a gap between the frame and the bottom of steel main girders. Representing these gaps in the model is difficult because their arrangement is essentially random. Moreover, the support susceptibility of individual girders is variable.

In the FEM model, the span structure was assumed to be a flat grating with fixed support at the abutments and flexible support at the frame. Another complication in the bridge model is the representation of very light truss bracing between the beams, as visible in Figure 5b. For this reason, only the concrete deck slab was assumed in the FEM model to be involved in distribution of the loads between the girders. Its stiffness is  $EI_y = 4.5 \text{ MNm}^2$ . Based on the field test results, it was found to be  $EI_y = 8.5 \text{ MNm}^2$ , which was included in the corrected FEM model, after the transport which is the subject of this paper passed the bridge.

The position of the vehicle in the cross-section of the bridge also has a significant influence on deflections. This is illustrated in the graphs given in Figure 15, representing the situation, when there is a full load on the span. For deflection prediction it was assumed that the load passage

takes place along central line of the span, i.e., the trailer is in the middle between both edges of the span. Moreover, both steel supports represent moderate stiffness for instance due to not-ideal restriction of horizontal movement of their feet (against horizontal forces). This situation is represented by black line (MES). The biggest deflection (calculated, before any measurements) was found to reach about 20 mm. Actually, the following differences from the model were found due to results of measurements:

- The first set of axles was running more than 80 cm from the central line of the span towards beam no. 8, due to the maneuvers of the vehicle on a bend along the approach before the bridge, (manoeuvres not taken into account in very first analysis) – red line in Figure 15;
- The second set of axles was running almost 30 cm from the central line of the span towards beam no. 1, due to the maneuvers of the vehicle – blue line in Figure 15;
- The second set of axles was probably slightly lighter than the first one;
- The stiffness of both steel supports was slightly higher than assumed;
- Transversal stiffness of the span was bigger than assumed.

The curve 'MES' was prepared before any measurements, having the limited knowledge about stiffness of the span and supports. The curves ' $e = -0.29$  m' and ' $e = 0.86$  m' were calculated knowing the position of both sets of wheels on the bridge and knowing the actual (measured

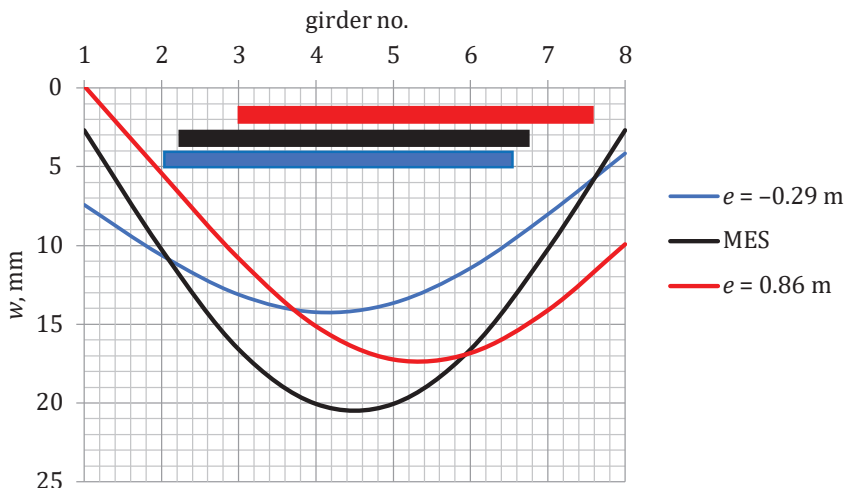


**Figure 15.** Distribution of (calculated) deflections of the main beams in the cross-section with measurement points C and E

during heavy cargo passage) deflection of beam no. 4 at point C as well as the actual deflection of beam no. 8 at point E.

Thus, theoretical value of the largest deflection of the main span was expected to reach about 20 mm – according to results of computer calculations. The same deflection – according to the results of simplified “manual” calculations, assuming the lack of rigid connection (integration) between the concrete deck slab and steel girders and assuming that two girders under the sidewalks (no. 1 and no. 8) are not involved at all in load carrying – was about 30 mm (roughly). According to the measurements the maximal deflection reached about 15 mm (see Section 4), for both sets of axles. When actual position of both sets of axles and actual stiffness of the span and steel supports were taken into account during after-passage computer calculations, the theoretical deflection was about 17 mm for the first set of axles and about 14 mm for the second set of axles.

## 6. Passing the bridge by road transport of ‘unknown’ weight

Not only self-propelled trailers but also units composed of tractor and trailer, pass the considered bridge, from time to time. In the latter case the axle loads are lower than loads appeared when the wash tower was transported on a special self-propelled trailer. Figure 16 shows a certain cargo together with a tractor-trailer combination vehicle. This heavy load passed the bridge several hours before the wash tower was transported, which is described in Section 4. The structural safety analysis referring to this passage was a task of another group of engineers, so authors did not know the weight of a cargo. However, the measurement system was ready thus it was a good (but unexpected) opportunity to resolve of ad hoc formulated task, i.e., to find the weight of the heavy transport. It was also a good opportunity to test the measurement equipment.

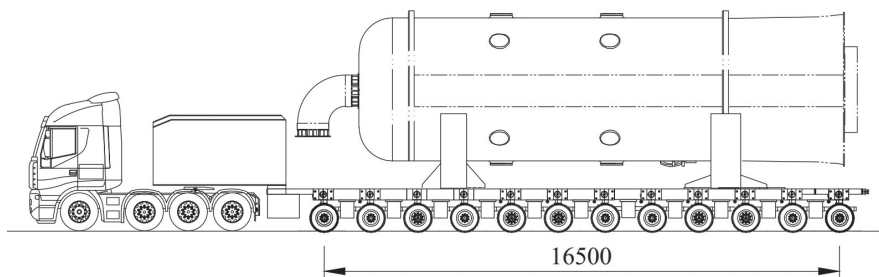
As in the case of the previously described transport, the deflections of the bridge were measured during this crossing. The measuring setup previously described for the transport of wash tower, was used for this purpose.

Figure 17 shows the results of deflection measurement during the passage of the load. First the tractor entered the bridge and was moving from point H towards point O (Figure 13). When the tractor exited the bridge, and so the span was loaded only by the trailer, the structure and load diagram shown in Figure 13 could be used. Based on the graph of

the ratio of deflection functions  $w_C(t)$  and  $w_E(t)$  (i.e.,  $r(t)$ ), shown in Figure 18,  $n = 5.6$  was assumed. Therefore, the uniformly distributed load when axle load is  $P$ , axle spacing  $a = 1.5$  m and  $n = 5.6$  amounts to:

$$p = \frac{P}{n \cdot a} = \frac{P}{5.6 \times 1.5} = \frac{P}{8.4} \text{ [kN/mb]}. \quad (11)$$

The results of the measurements carried out during the passing of the wash tower, i.e., the determined (validated) beam parameters and the measured deflection of point C ( $w_C = 15$  mm at  $p = 44$  kN/m) were used in the calculations. For the measured deflection under the calculated load of 44 kN/m and for the maximum deflection ( $w_C = 3.913$  mm, Figure 17) measured during the crossing of the transport of 'unknown' weight (Figure 16) from Equation (10) one gets the axle load:



**Figure 16.** Industrial installation component loaded onto multi-axle trailer with road tractor

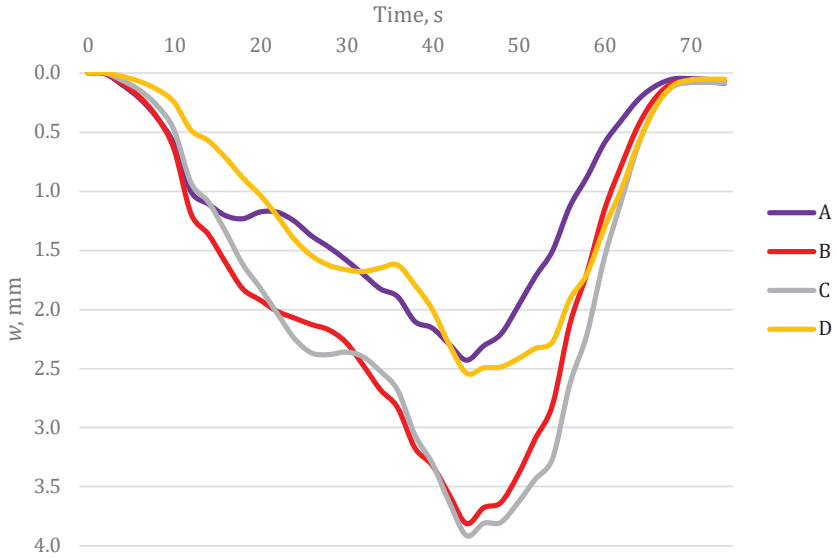


**Figure 17.** Deflections of measuring points during passing of load shown in Figure 16

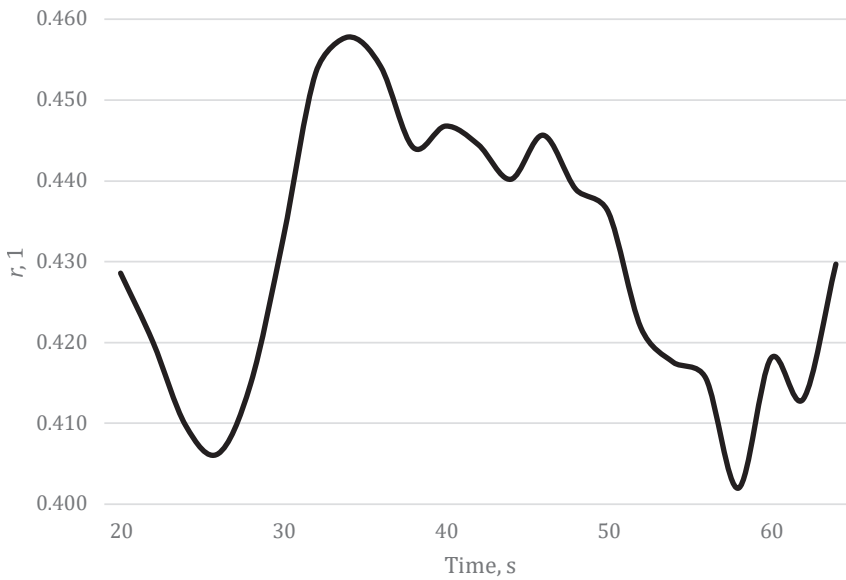


**Figure 18.** Locally measured deflections of points C and E as function  $r(t)$  during bridge crossing by transport shown in Figure 16

$$P = \frac{3.913}{15} \times 44 \times 8.4 = 96.4 \text{ kN}, \quad (12)$$

where  $3.913/15$  is a deflections quotient.

Having axle load  $P$  one can calculate the load's total weight distributed among the 18 axles (without the tractor):

$$Q = 18 \cdot P = 18 \times 96.4 = 1735 \text{ kN} \quad (13)$$

The weight is similar to that of the other frequent abnormal transports whose diagrams are shown in Figure 3.

## 7. Transport of gas turbine

Another load transported via the analysed bridge was a gas turbine (Figure 19). Similarly, as in the case of the wash tower, a special self-propelled trailer was used for this purpose. No deflection measurements were conducted during the passage of the gas turbine. However, using the structure model validated by the measurements of deflections during the wash tower passing one can simulate the deflections of points A, B, C, D during the crossing the bridge by the gas turbine. The loading diagram in this case was similar to that of one of the members of the wash tower transport unit. The total weight of this load (Figures 19 and 20) amounted to  $Q = 6360 \text{ kN}$ , which at 18 vehicle axles gives axle load  $P = 353.3 \text{ kN}$ . The overall load length amounted to  $L_0 = 25 \text{ m}$ . At a certain stage of the passage, the bridge was loaded over its whole length with the vehicle axles.

The load intensity for the considered girder, when  $n$  is similar as in Equation (10), defined as a uniformly distributed load amounts to:

$$p = \frac{P}{n \cdot a} = \frac{353.3}{6.04 \times 1.4} = 41.78 \text{ kN/m} \quad (14)$$

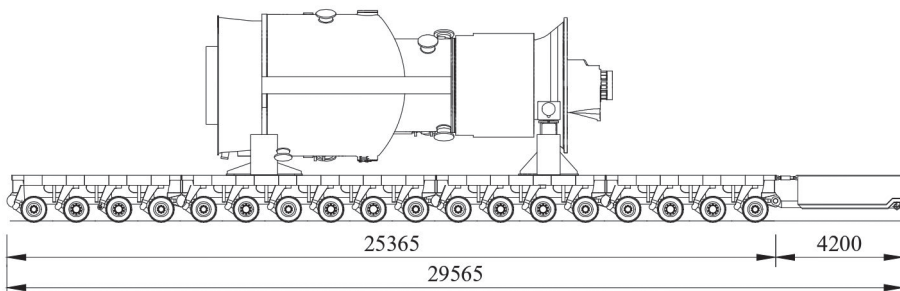


Figure 19. Loading diagram with cargo (gas turbine)

The above value is lower than the load induced by the vehicle shown in Figure 7 (in the case of the wash tower transport the distributed load amounted to  $p = 44 \text{ kN/m}$  (per one girder)).

Since the geometrical arrangement of axles is simpler than in the vehicle shown in Figure 7, as there is only one set of axles, bridge crossing was assumed to proceed uniformly. Hence the displacement graphs are less complicated (Figure 21). Instead of the time variable, distance variable was employed. First axle position  $x$  equals to 0 when



**Figure 20.** Bridge crossing by special transport unit with gas turbine

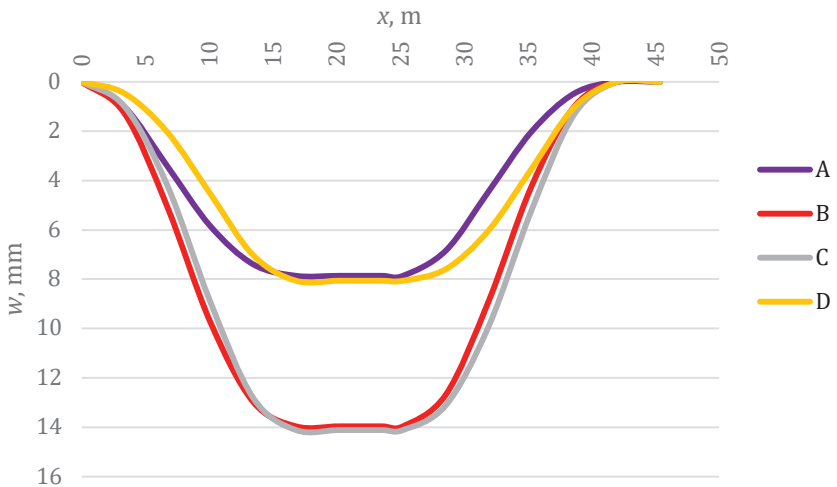


**Figure 21.** Simulated graph of deflection during bridge crossing by gas turbine

the first axle is over the abutment bearing. Therefore, when the load takes up interval H-A (Figure 13),  $x = 3.60$  m and when the span is fully loaded, then  $x = L = 16.8$  m. Since the load length amounts to  $L_0 = 25$  m and it is greater than the bridge length, when  $x > L$  the deflection stabilizes during the passage of the transport unit. Obviously when  $x > 25$  m the vehicle begins to exit the bridge. The bridge will be fully unloaded when  $x = 42.0$  m.

## 8. Operational load

The bridge had been strengthened and adapted to carry very heavy loads. An element of the strengthening are intermediate steel piers. However, when typical light loads (passenger cars or light trucks) appear on the span the latter rests mainly on the abutments and the loads only to a minimum degree are transmitted to the intermediate supports.

The loading of the bridge by standard motor vehicles is so light that the steel frame piers are not loaded at all. A clearance amounting to about 1–2 mm occurs between the girders and the frame supports. This configuration of the structure is put to the test below. Two vehicles T4 (Figure 1) driving in opposite directions and passing each other on the bridge (Figure 22) were assumed as the maximal operational load. A single motor vehicle weighing 443.8 kN whose specifications are presented in Figure 1 was assumed as the minimal operational load.

When the bridge roadway is loaded as in Figure 22, the axle load of the aligned two rear axles at midspan for number of girders taking part in load carrying  $n = 5.4$  (calculated on the basis of the predicted load distribution among girders C and E) amounts to:

$$P = \frac{2 \times 122.8}{5.4} = 45.5 \text{ kN (per girder)}. \quad (15)$$

Thus, the axle load is roughly one-and-a-half-fold lighter than for special transports since in the case of the wash tower it amounted to  $372/6 = 62$  kN/axle (per one main girder), where 6 is the number of girders taking part in load carrying. The results of the deflection calculations are compared in Table 1. It appears that the deflections over a frame pier when the span behaves as a simply supported beam considerably exceed 1–2 mm (i.e., the gap over the frame support). This observation also applies to the load in the form of a single four-axle motor vehicle T4 (see Figure 1), as in this case  $w_F > 1$  mm. Therefore, cases of loading with heavy goods vehicles should be also analysed for the load diagram presented in Figure 13, i.e., with the participation of the steel intermediate supports.

In addition, the maximal deflection at the midspan of the bridge is given in column BC. A comparison of deflections  $w(2T4)$  induced by two vehicles T4 and deflection  $w(WT)$  caused by the wash tower transport (see Figure 7) shows that the latter deflection is several-fold greater:

$$ws = \frac{w(WT)}{w(2T4)} = \frac{15}{4.7} = 3.2. \quad (16)$$

Table 1. Calculated deflections of girder No. 4 in measuring points, induced by vehicles T4

Load diagram		Deflections in measuring points, mm					
		A	B	BC	C	D	F
without taking into account steel frame supports	2T4	6.899	10.495	10.864	10.227	6.485	4.303
	T4	5.014	7.916	8.386	8.080	5.318	3.556
taking into account steel frame supports		2.925	4.650	4.731	4.258	2.274	1.375

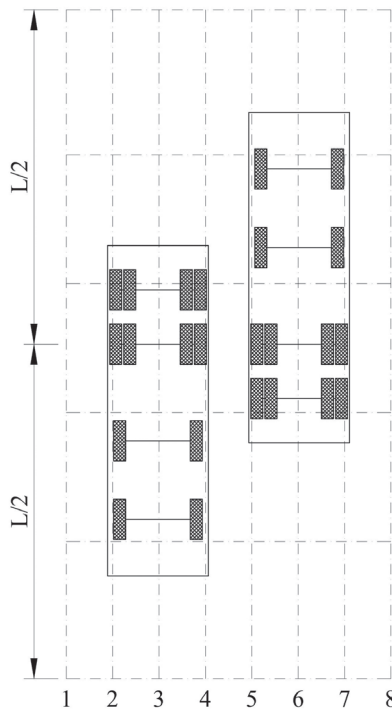


Figure 22. Arrangement of vehicles T4 on bridge roadway. Positions of main girders are denoted with numbers 1–8

## Conclusions

A case of a bridge adapted to carrying considerable loads, located in a network of ordinary city streets but on a route used for transporting heavy cargos from a riverside to a large and expanding industrial plant has been presented. Knowing the axle loads of the heaviest monitored transport (of a wash tower) the deflections of the bridge's span under a considerable load were measured using simple measuring devices (inductive sensors). Consequently, the actual stiffness of the structure was determined and at the same time the integration of the main girders with the reinforced concrete deck slab was verified. Some general or detailed conclusions are listed below.

- Very heavy cargo abnormal transport cannot pass through ordinary bridges if they are not strengthened enough, as in presented case study, even they are designed for the largest but standard loads.
- The largest and the heaviest cargo loads are distributed into numerous axles and numerous wheels (sometimes more than 100) and this way the whole load can be considered as uniformly distributed load. The value of such loads is bigger than  $50 \text{ kN/m}^2$ , i.e., it is much more than value of distributed load considered in many standards.
- If there is a weak bracing between the girders, the position of the vehicle on the deck is significant for the actual load distribution between the girders. In the presented case study, the deflections of side girders (under the sidewalks) are much smaller than the deflections of main girders located under the bridge road, even though the width of the trailer is relatively large.
- The maximum deflection estimated in simplified, roughly way was about 30 mm. The same calculated with computer method was about 20 mm, the measured deflection reached about 15 mm. The differences had their source mainly in the lack of certainty regarding the cooperation of the steel girders and the deck slab as well as the transverse stiffness of the span. Moreover, the weight of the biggest element (wash tower) after the weighing during loading on a trailer was found to be slightly smaller than declared.
- The deflection almost disappeared after the load had exited the bridge.

The presented case study also proves that it is possible to calculate the axle loads of vehicles based on weigh-in-motion measurements of span deflections and provides a description of the adaptation of a bridge to carrying very heavy loads which usually do not occur in a road network. The bridge had been adapted to carrying considerable

loads many years before the transports described in this paper were conducted. Nevertheless, the adaptation proved to be effective enough to enable the crossing of the bridge by many different abnormal transports whose total weight and axle loads were very heavy in some cases.

## REFERENCES

- European Guidelines. (2006). *European best practice guidelines for abnormal road transports*. European Commission – Directorate-General for Energy and Transport. [https://road-safety.transport.ec.europa.eu/system/files/2021-07/abnormal\\_transport\\_guidelines\\_en.pdf](https://road-safety.transport.ec.europa.eu/system/files/2021-07/abnormal_transport_guidelines_en.pdf)
- Gnap, J., Jagelčák, J., Marienka, P., Frančák, M., & Vojteková, M. (2022). Global assessment of bridge passage in relation to oversized and excessive transport: Case study intended for Slovakia. *Applied Sciences*, 12(4), Article 1931. <https://doi.org/10.3390/app12041931>
- Godavarthy, R. P., Russell, E., & Landman, D. (2016). Using vehicle simulations to understand strategies for accommodating oversize, overweight vehicles at roundabouts. *Transportation Research Part A: Policy and Practice*, 87, 41–50. <https://doi.org/10.1016/j.tra.2016.03.002>
- Hammada, A., Nims, D., Hunt, V., Commander, B., & Helmicki, A. (2013). Superload evaluation of the Millard Avenue Bridge over the CSX railroad. *Proceedings of Transportation Research Board Annual Meeting*, Washington, D.C., USA. [https://www.researchgate.net/publication/257921554\\_Superload\\_Evaluation\\_of\\_the\\_Millard\\_Avenue\\_Bridge\\_over\\_the\\_CSX\\_Railroad](https://www.researchgate.net/publication/257921554_Superload_Evaluation_of_the_Millard_Avenue_Bridge_over_the_CSX_Railroad)
- Helmi, K., Bakht, B., & Mufti, A. (2014). Accurate measurements of gross vehicle weight through bridge weigh-in-motion: A case study. *Journal of Civil Structural Health Monitoring*, 4, 195–208. <https://doi.org/10.1007/s13349-014-0076-5>
- Hildebrand, M., Biliszczyk, J., & Berger, A. (2008). Monitoring system for a cable-stayed bridge in Plock. *17th Congress of IABSE, Chicago, Creating and Renewing Urban Structures*, Chicago, USA, 554–555. <https://doi.org/10.2749/222137908796293785>
- Lydon, M., Taylor, S. E., Robinson, D., Mufti, A., & Brien E. J. O. (2016). Recent developments in bridge weigh in motion (B-WIM). *Journal of Civil Structural Health Monitoring*, 6, 69–81. <https://doi.org/10.1007/s13349-015-0119-6>
- Machelski, C., & Hildebrand, M. (2015). Efficiency of monitoring system of a cable-stayed bridge for investigation of live loads and pier settlements. *Journal of Civil Structural Health Monitoring*, 5, 1–9. <https://doi.org/10.1007/s13349-014-0074-7>
- Machelski, C., & Hildebrand, M. (2021). Cable-stayed bridge loads caused by traffic congestion on the deck measured with bridge monitoring system. *Baltic Journal of Road and Bridge Engineering*, 16(2), 66–89. <https://doi.org/10.7250/bjrbe.2021-16.524>

- Macioszek, E. (2020). Oversize cargo transport in road transport – Problems and issues. *Sci. J. Silesian Univ. Technol. Ser. Transp.*, 108, 133–140.  
<https://doi.org/10.20858/sjsutst.2020.108.12>
- Mohammed, O., González, A., & Cantero, D. (2018). Dynamic impact of heavy long vehicles with equally spaced axles on short-span highway bridges. *The Baltic Journal of Road and Bridge Engineering*, 13(1), 1–13.  
<https://doi.org/10.3846/bjrbe.2018.382>
- Onysyk, J., & Hildebrand, M. (1999). Static schemes of overweight transports and bridge stress intensity. Issues relating to the design, construction and maintenance of small bridges. Dolnośląskie Wydawnictwo Edukacyjne, Wrocław (in Polish).
- Orkisz, J. (1998). Finite difference method. In M. Kleiber (Ed.), *Handbook of computational solid mechanics* (Part III). Berlin: Springer-Verlag.
- Petru, J., & Krivda, V. (2017). Height and width parameters for ensuring passage of excessive loads on roads. *Acta Polytechnica*, 57(3), 209–217.  
<https://doi.org/10.14311/AP.2017.57.0209>
- Petru, J., & Krivda, V. (2021). The transport of oversized cargoes from the perspective of sustainable transport infrastructure in cities. *Sustainability*, 13(1), Article 5524. <https://doi.org/10.3390/su13105524>
- Vrábel, J., Loman, M., Pa'lo, J., Šarkan, B., & Hudcovský, A. (2022). Evaluation of the safety of overweight and/or oversized traffic based on the analysis of lateral acceleration during transport. *IOP Conf. Series: Materials Science and Engineering*, 1247, Article 012040.  
<https://doi.org/10.1088/1757-899X/1247/1/012040>
- Wood, S. M., Akinci, N. O., Liu, J., & Bowman, M. D. (2007). *Long-term effects of super heavy-weight vehicles on bridges*. Joint Transportation Research Program FHWA/IN/JTRP-2007/10, Final Report, Purdue University, West Lafayette, Indiana, USA. <https://docs.lib.purdue.edu/jtrp/236/>
- Yudhistira, A. T., Fajar, A. S., Hud, I. N., Suanda, B., & Awaludin, A. (2022). Structural condition assessment of a log bridge under heavy traffic load (Case study: 105 tons gas engine delivery in Central Borneo project). In S. Belayutham, C.K.I. Che Ibrahim, A. Alisibramulisi, H. Mansor, & M. Billah (Eds.), *Proceedings of the 5th International Conference on Sustainable Civil Engineering Structures and Construction Materials, SCESCM 2020. Lecture Notes in Civil Engineering*, 215, 669–684, Springer, Singapore.  
[https://doi.org/10.1007/978-981-16-7924-7\\_44](https://doi.org/10.1007/978-981-16-7924-7_44)